Supporting Information

Investigations of the Key Macrolactamisation Step in the Synthesis of Cyclic Tetrapeptide Pseudoxylallemycin A

Alan J Cameron[a,b,c], Christopher J. Squire[c], Ashley Gérenton[a,c], Louise A. Stubbing[a,c], Paul W. R. Harris[a,b,c], and Margaret A. Brimble[a,b,c]*

[a]*School of Chemical Sciences, The University of Auckland, 23 Symonds St, Auckland 1010, New Zealand*

[b]*The Maurice Wilkins Centre for Molecular Biodiscovery, The University of Auckland, Private Bag 92019, Auckland 1010, New Zealand*

[c]*School of Biological Sciences, The University of Auckland, 3A Symonds St, Auckland 1010, New Zealand*

E-mail: m.brimble@auckland.ac.nz

Table of contents

Crystallography

Peptides **1**, **1***, **7**, and **9** were crystallised by controlled evaporation from solvent systems listed in Table S2. Crystals were coated in a mixture of 70% Paratone N and 30% mineral oil, mounted in nylon loops and flash cooled in liquid nitrogen for transport to the Australian Synchrotron. Data were collected on the MX2 beamline at the Australian Synchrotron at 100K and at a wavelength of 0.71073 Å [1]. Data were processed using XDS and the unmerged intensity data converted to SHELX hkl format using XDSCONV [2]. The structures were determined using SHELXT [3]. The models were refined initially isotropically, and finally anisotropically by least squares refinement using SHELXL [4]. Solvent molecules and idealised hydrogens in riding positions were included in final rounds of refinement. Each structure contains a single peptide molecule with varying solvent molecules included. Disorder in the peptide **9** structure was modelled by two completely overlapping conformations. X-ray crystallography data collection and refinement statistics are provided in Table S2. Crystal structures were deposited in the Protein Data Bank with ID codes, 6MW1, 6MW2, 6MVZ, 6MW0.

Cyclisation of peptide 8

As expected from our previous work,[5] attempts to cyclise the alternate linear pre-cursor **8** proved unsuccessful, with predominantly unidentified side-products, unreacted **8**, and minimal formation of **1** with T3P in DMF (**Table S1**, entry 2). However, using PyAOP and 1 % v/v DIPEA (**Table S1**, entry 1) the reaction proceeded to completion in less than 4 h, but the product mixture was dominated by a later eluting species formed through cyclodimerisation (MS (ESI+): *m/z* $[M+H]^+$ calculated for $C_{64}H_{88}N_8O_8$: 1097.68; observed 1097.6). Fairweather *et al,*[6] employing a pseudoproline turn inducing strategy, were able to synthesise eight cyclic tetrapeptides in good to moderate yields, including cyclo(Leu-Ser)$_2$ in 66 % yield from its corresponding Ser($\Psi^{Me,Me'}$-Pro) derivative. NMR investigations of the peptide H_2N-(Phe-Ser($\Psi^{Me,Me'}$-Pro))$_2$-COOH revealed $C^{\alpha}_{i}H$ - C^{α}_{i+1H} NOEs in accordance with a *cis-trans-cis* (*ctc*) conformation, further confirmed by crystallography. Somewhat surprisingly, while this series of compounds more closely resemble linear peptide **8** in their relative positions of *N*-alkylation, we found peptide **8** to be the less favourable cyclisation precursor (relative to **7**), suggesting it does not adopt a similar *ctc* conformation. In fact, the pseudoproline strategy appears superior at inducing conformations that are predisposed to cyclisation with comparison to both *N*-methylation (our findings - peptide **8**) and proline itself, with Haddai *et al* [7] finding H_2N-(Leu-Pro)$_2$-COOH to cyclise in poor yield with significant epimerisation.

Table S1: Attempted synthesis of pseudoxylallemycin A (**1**) by cyclisation of linear peptide **8**.

entry	Reagent (equiv).	Base (equiv.)	Temp °C	Solv (1 mM)	% **1***: **1** [a]
1	PyAOP (3)	DIPEA (1 % *v/v*)[b]	25	DMF	cd-0:100
2	T3P (3)	DIPEA (6)	45	DMF	np-m

[a] np-m indicates no desired product formation but a large number of unidentified peaks were observed; cd- indicates the cyclodimer was the predominant species formed. Ratio based on % area measured at 214 nm on Waters Alliance analytical HPLC employing a gradient of 30 – 80 % Solvent B over 30 minutes and flow rate of 1 mL/min on a Phenomenex Luna C18 5µm 4.6 mm x 250 mm column operated at room temperature. Solvent A = 100 % H_2O + 0.1 % TFA. Solvent B = 100 % MeCN + 0.1 % TFA. In all cases (except for BTC reactions), peptides were diluted to 1 mM and incubated for 15 min at the prescribed temperature before addition of base, followed by the coupling reagent.

Aqueous stability tests of cyclic intermediates formed during cyclisation of peptide 7

Three experiments were performed to test the aqueous stability and reactivity of the kinetic intermediates formed during the optimised T3P mediated cyclisation of **7** in DMF. It appeared that the anionic coupling reagent by-products were superior nucleophiles as compared to water, with the addition of 10 % *v/v* water to the reaction mixture after 10 minutes having little or no effect upon reaction progression to **1** and **1*** (Table 1, entry 24). However, in the presence of hydroxide nucleophiles (0.3 % *v/v* 1M NaOH, final) hydrolysis of the intermediates to linear peptide **7** was observed over 5 hours (Table S1, entry 25). Addition of 10 % *v/v* aliquot of a 1:1 water and acetonitrile mixture containing TFA (0.3 % *v/v* final) instead resulted in rapid degradation (< 1 h) to linear peptides **7** and **9**, analogous to storage in HPLC eluent (Table 1, entry 26).

Also noteworthy is that although linear peptide **9** cyclises to **1*** without epimerisation using PyAOP and more concentrated base (Table 1, entry 27), when employing our optimised T3P conditions for this peptide (Table 1, entry 28) a small amount of epimerisation is observed, with a ratio of **1*** to **1** of 88:18. This T3P cyclisation of **9** also proceeded via two intermediate peaks (in an approx. 1:1 ratio) which were not observed during its rapid cyclisation with PyAOP.

Data Tables

Table S2: Comparison of the ^{1}H and ^{13}C NMR spectroscopic data of synthetic and isolated pseudoxylallemycin A(**1**).[8]

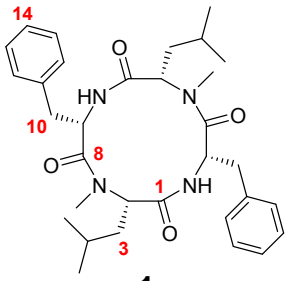

1

	1 (500 MHz, DMSO-d_6, 298K)		**Lit.**[8] (500 MHz, DMSO-d_6, 293K)	
position	δ_C	δ_H, mult. (*J* in Hz)	δ_C	δ_H, mult. (*J* in Hz)
1	169.5, qC	-	169.6, qC -	-
2	58.2, CH	3.84, dd (11.6, 3.50)	58.3, CH	3.83, m
3a	36.5, CH_2	1.35, m	36.6, CH_2	1.34, m
3b	-	1.57, m	-	1.55, m
4	24.3, CH	1.22, m	24.4, CH	1.21, m
5	20.8, CH_3	0.75, d (6.5)	20.2, CH_3	0.74, d (6.4)
6	23.1, CH_3	0.83, d (6.6)	23.2, CH_3	0.83, d (6.4)
7	30.6, CH_3	2.59, s	30.2, CH_3	2.57, s
8	171.6, qC	-	171.8, qC	-
9	50.8, CH	4.82, m	50.9, CH	4.81, m
10a	37.7, CH_2	2.67, m	37.7, CH_2	2.67, dd (12, 7.4)
10b	-	3.18, dd (14.4, 6.1)	-	3.17, dd (12, 5.0)
11	137.9, qC		138.2, qC	-
12	129.6, CH	7.16, d (7.7)	129.7, CH	7.15, d (7.8)
13	127.8, CH	7.23, t (7.5)	127.9, CH	7.22, t (7.8)
14	126.0, CH	7.15, t (7.3)	126.2, CH	7.14, t (7.3)
15	127.8, CH	7.23, t (7.5)	127.9, CH	7.22, t (7.8)
16	129.6, CH	7.16, d (7.7)	129.7, CH	7.15, d (7.8)
NH(1)		8.10, br d (7.8)		8.18, br d (8.1)

Table S3: Crystal data, data collection and structure refinement details are summarized below for compounds **7**, **9**, **1**, and **1***.

Data collection:	**7**	**9**	**1**	**1***
Sequence[a]	Mle-Phe-Mle-Phe	Mle-Phe-Mle-D-Phe	cyclo-Mle-Phe-Mle-Phe	cyclo- Mle-Phe-Mle-D-Phe
Solvent	EtOH/H_2O	MeOH/H_2O	MeOH/H_2O	MeOH/EtOH/THF/H_2O
Molecules in AU	1 + 1 TFA + 1 H_2O	1[e] + 2 MeOH + 6 H_2O	1 + 1 H_2O	1
Crystal description	colourless rod	colourless rod	colourless plate	colourless plate
	0.02 x 0.02 x 0.1 mm	0.02 x 0.03 x 0.2 mm	0.01 x 0.2 x 0.3 mm	0.02 x 0.1 x 0.2 mm
X-ray source	AS-MX2	AS-MX2	AS-MX2	AS-MX2
Wavelength (Å)	0.71075	0.71075	0.71075	0.71075
Temperature (K)	100	100	100	100
Resolution[b] (Å)	23.44 – 0.83 (0.85 – 0.83)	23.02 – 0.78 (0.80 – 0.78)	26.42 – 0.77 (0.79 – 0.77)	20.49 – 0.77 (0.79 – 0.77)
Space group	$P\,2_12_12_1$	$P\,2_12_12_1$	$P\,2_12_12_1$	$P\,2_12_12_1$
a, b, c ()	8.255, 19.173, 23.446	8.291, 20.931, 23.016	9.633, 12.706, 26.415	10.928, 13.552, 20.488
Unique reflections[b]	4332 (253)	4911 (268)	4124 (279)	3920 (290)
Redundancy[b]	14.3 (11.9)	11.5 (10.0)	11.9 (11.8)	11.4 (9.5)
Completeness[b] (%)	98.0 (83.8)	99.2 (92.0)	98.3 (91.7)	99.5 (95.1)
R_{merge}[b]	0.117 (0.127)	0.059 (0.567)	0.078 (0.141)	0.042 (0.093)
R_{pim}[abc]	0.033 (0.038)	0.019 (0.189)	0.024 (0.043)	0.013 (0.034)
I/σI[a]	22.9 (16.5)	14.7 (2.2)	27.0 (19.6)	32.1 (19.1)
CC1/2[bd]	0.989 (0.990)	0.999 (0.896)	0.993 (0.992)	0.999 (0.992)
Refinement:				
Resolution (Å)	23.44 – 0.83	23.02 – 0.78	26.42 – 0.77	20.49 – 0.77
SHELXL $R_{(int)}$	0.0785	0.0575	0.0811	0.0524
SHELXL $R_{(sigma)}$	0.0488	0.0371	0.0367	0.0282
SHELXL R1 $_{Fo>4sig(Fo)}$	0.0569	0.0891	0.0430	0.0407
SHELXL R1 $_{all\ data}$	0.0675	0.0985	0.0437	0.0424
PDB code	6MVZ	6MW0	6MW1	6MW2

[a] Mle represents NMe-Leu. [b] Numbers in parentheses are for the outermost shell. [c] R_{pim} = Precision-indicating *R* factor (see Weiss, 2001). [cd]CC1/2 = Correlation coefficient (see Karplus and Diederichs, 2012). [e] Disorder is modelled by two overlaid peptides each at 0.5 occupancy.

Characterisation of peptides

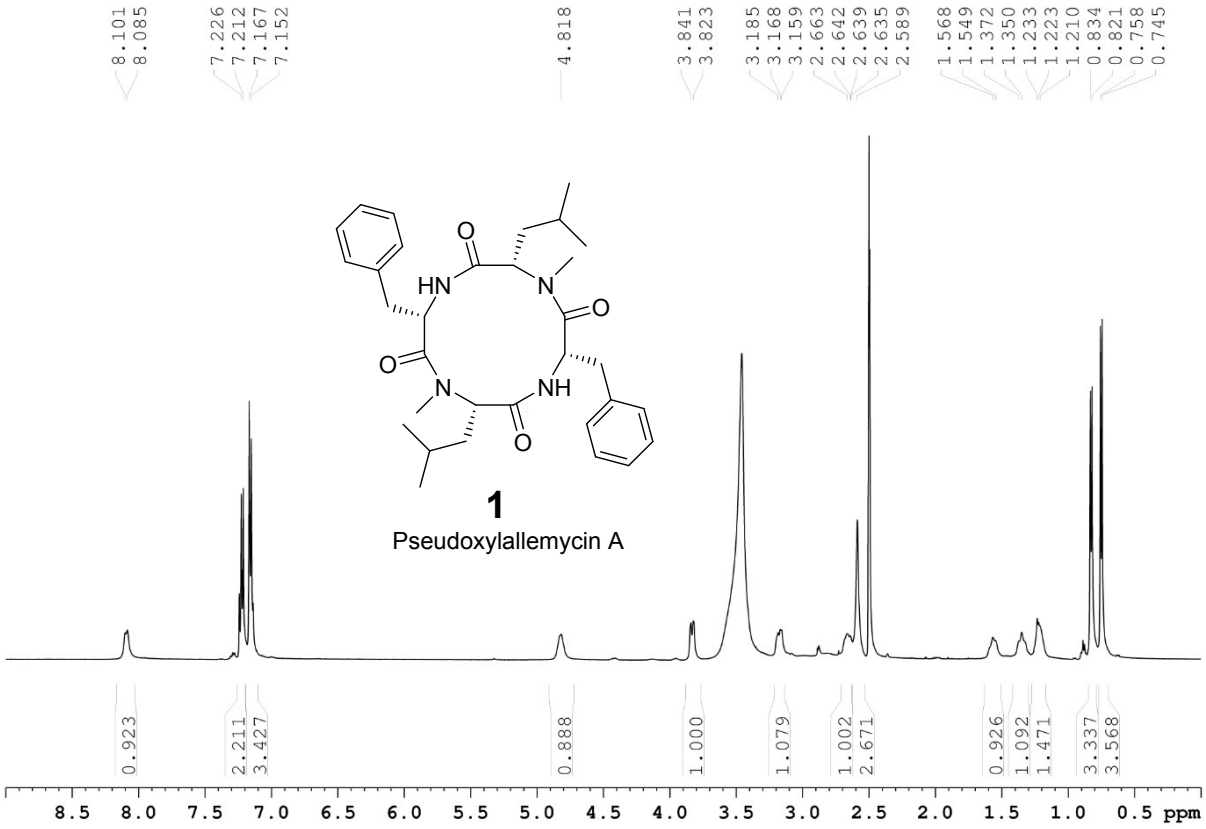

Figure S1: ^{1}H NMR spectrum of **1** (DMSO-d_6, 298 K, 500 MHz).

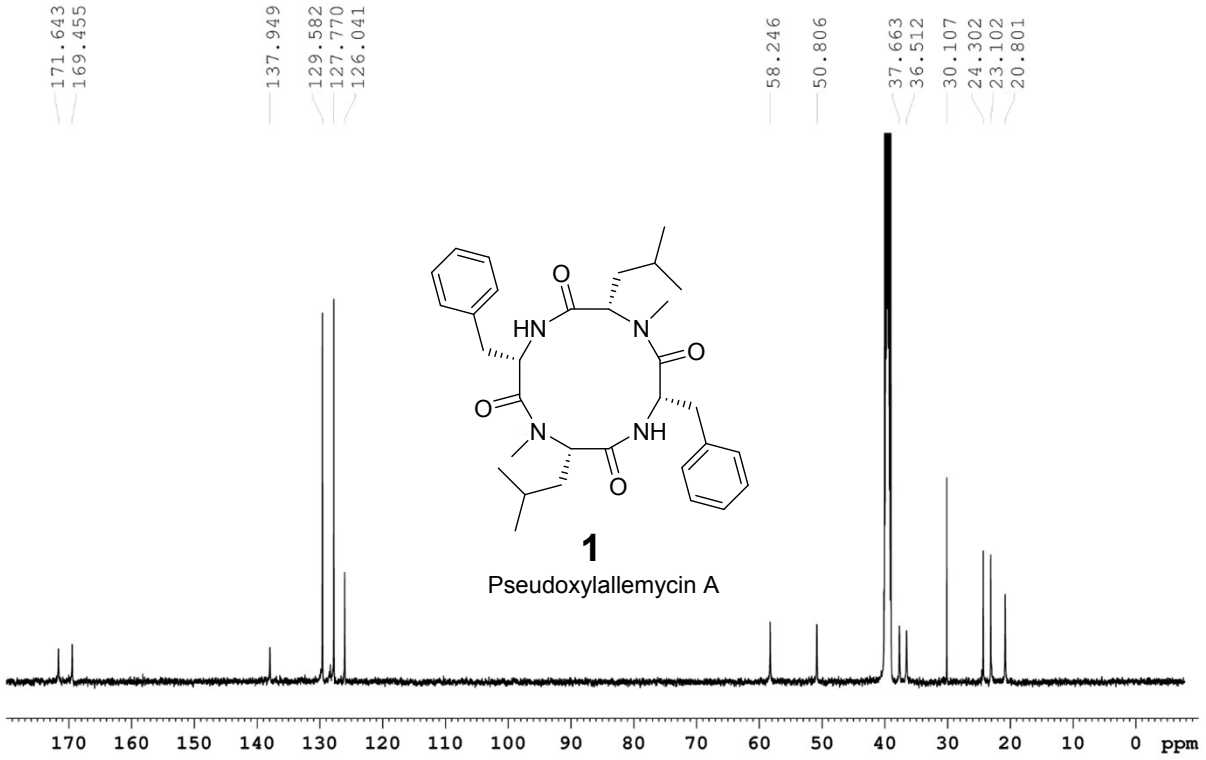

Figure S2: ^{13}C NMR spectrum of **1** (DMSO-d_6, 298 K, 125 MHz).

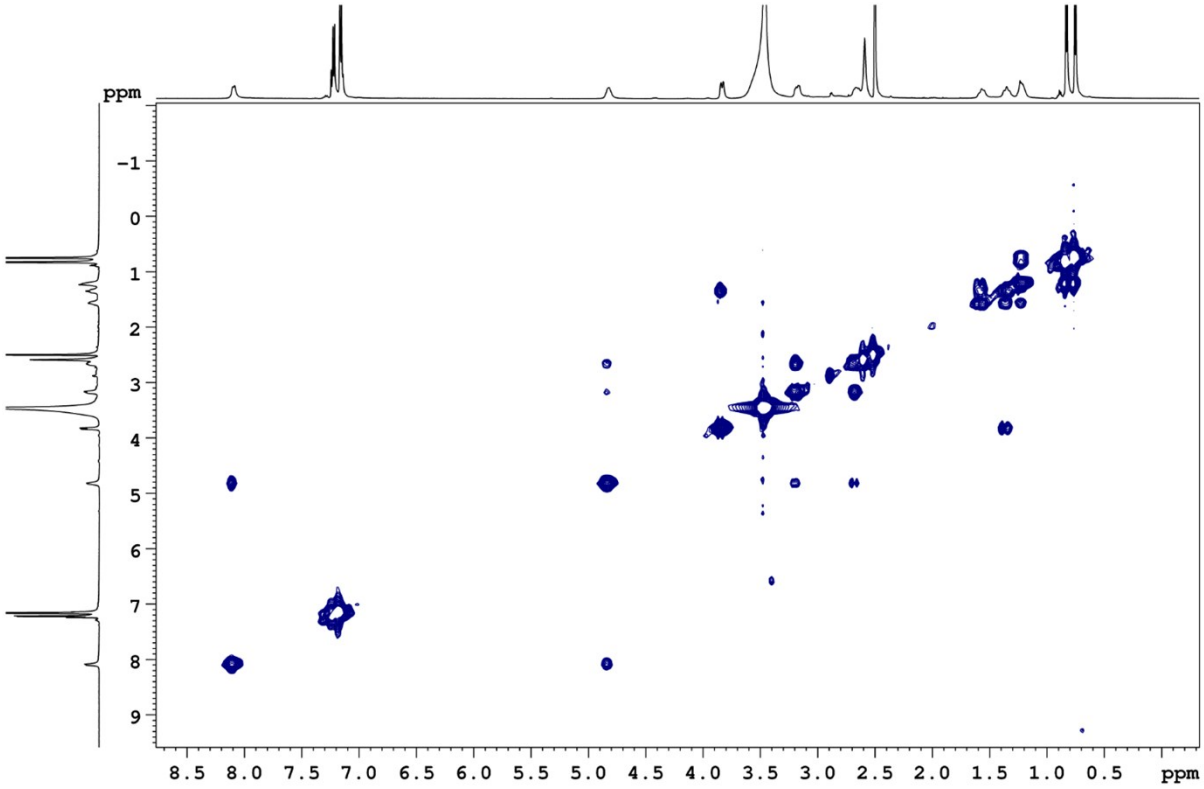

Figure S3: COSY spectrum of **1** (DMSO-d_6, 298 K, 500 MHz).

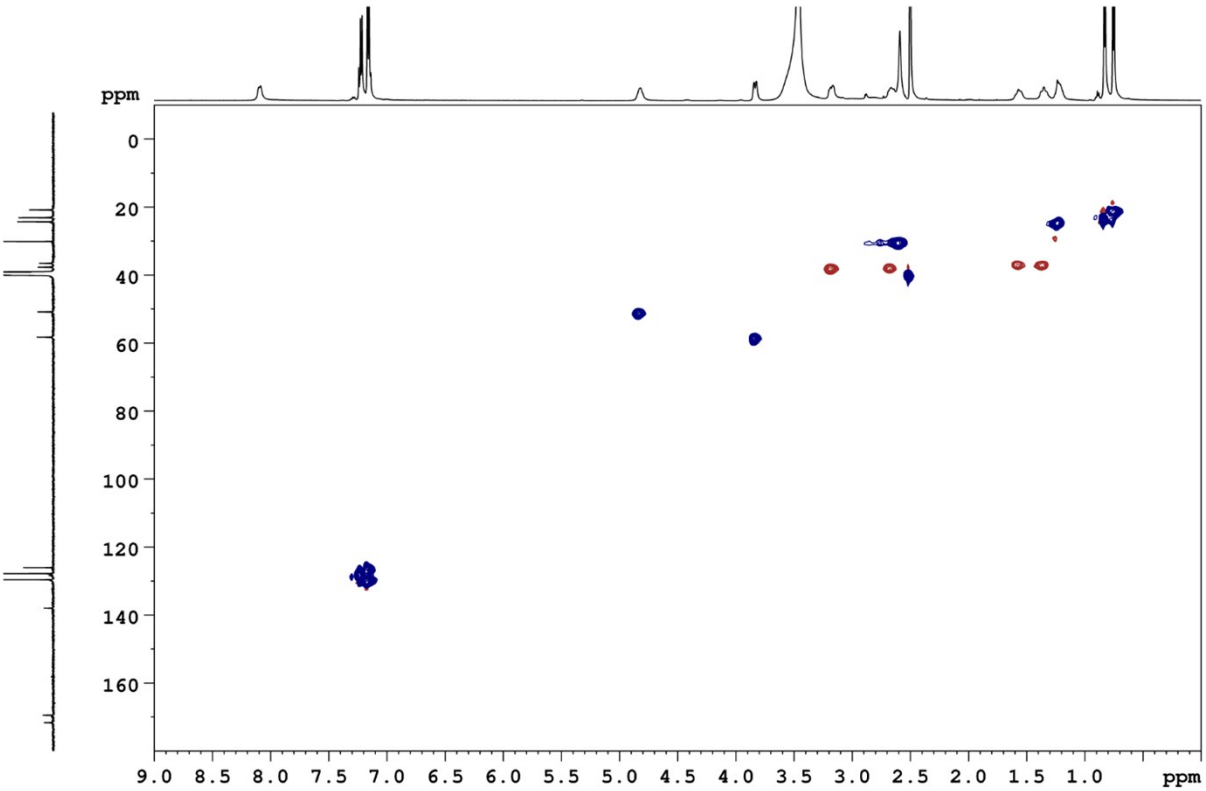

Figure S4: Edited HSQC spectrum of **1** (DMSO-d_6, 298 K, 500 MHz).

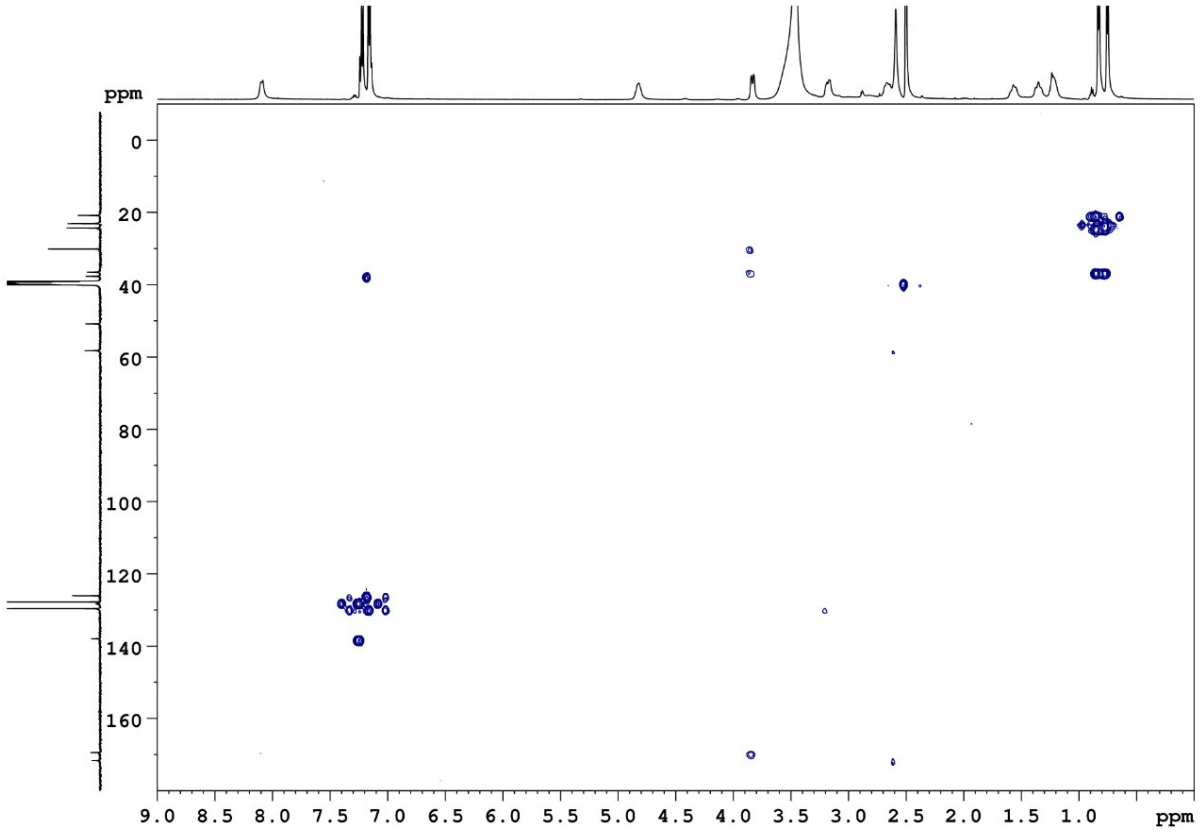

Figure S5: HMBC spectrum of **1** (DMSO-d_6, 298 K, 500 MHz).

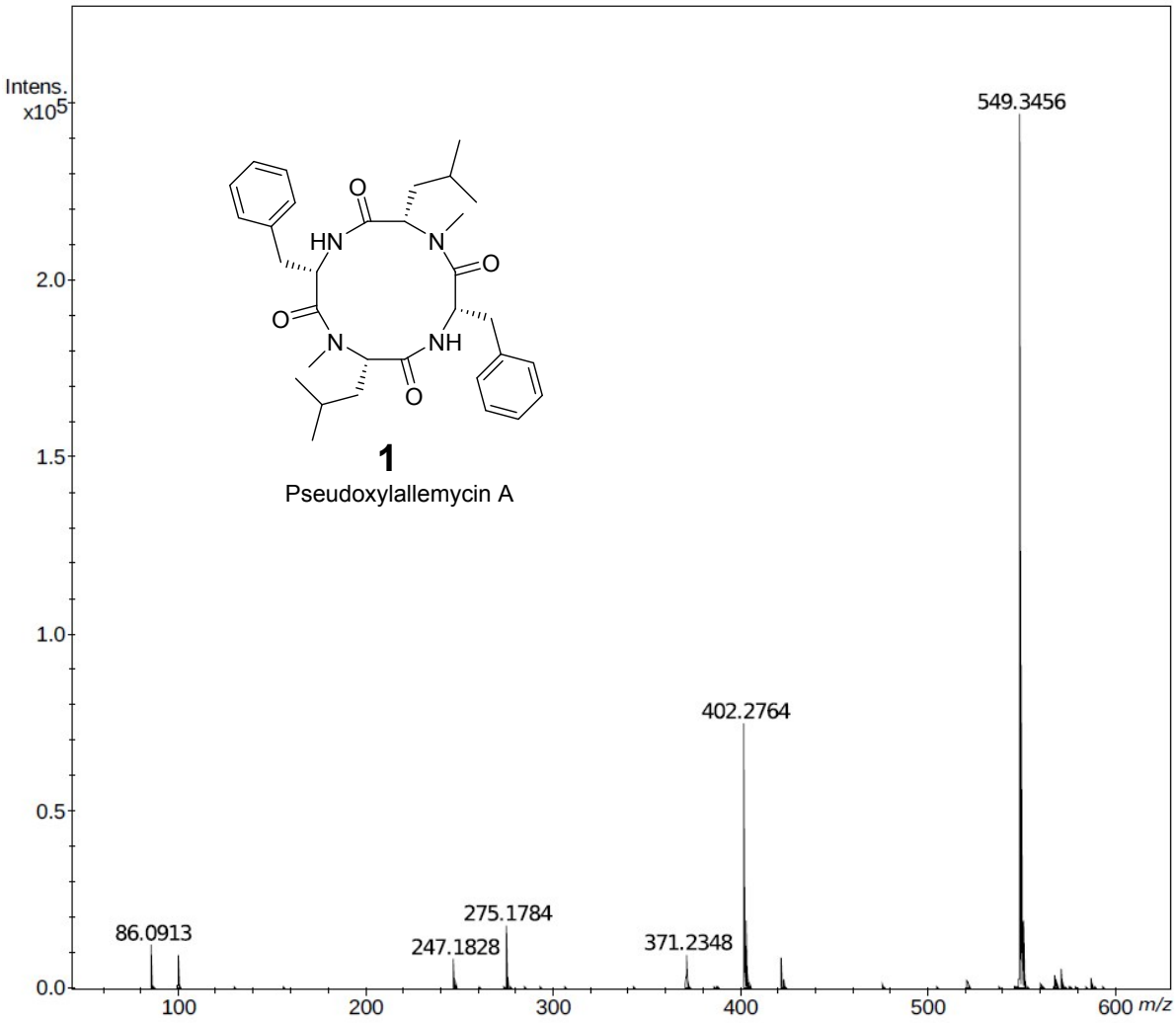

Figure S6: HRMS spectrum of **1**.

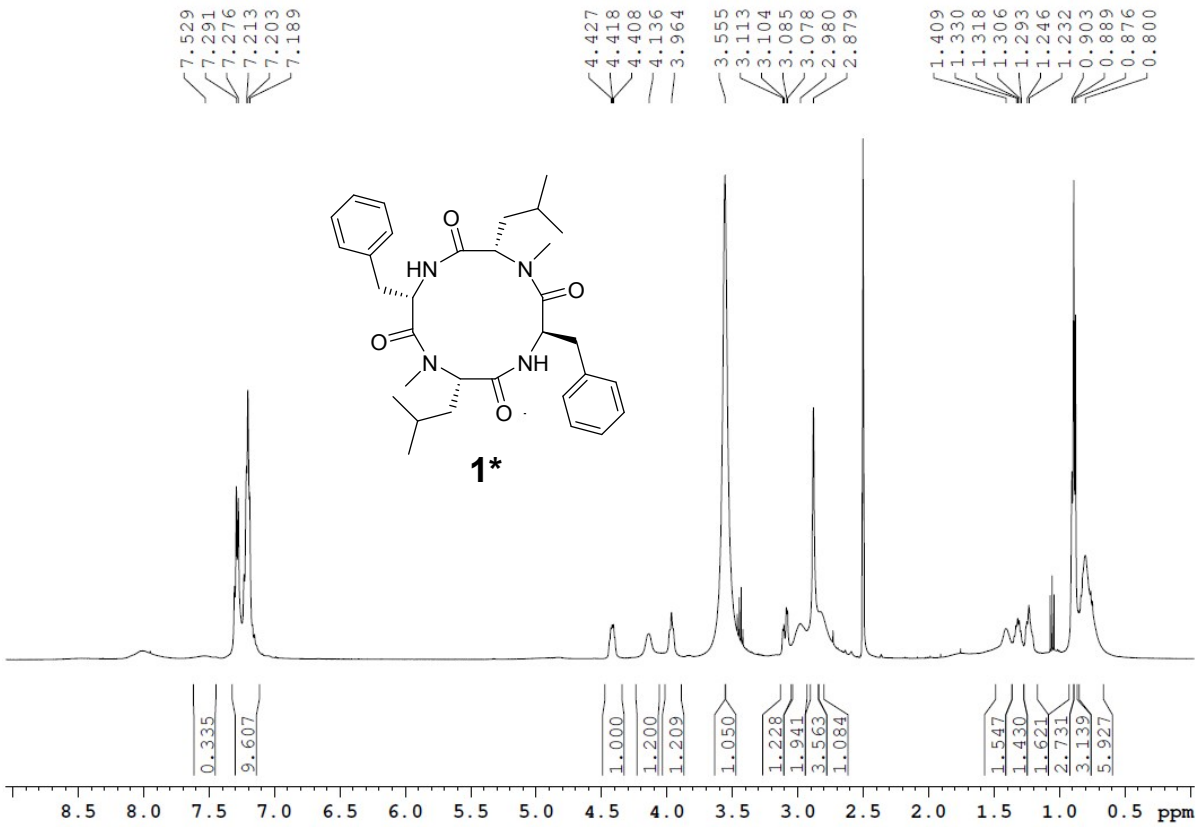

Figure S7: ^{1}H NMR spectrum of **1*** (DMSO-d_6, 298 K, 500 MHz).

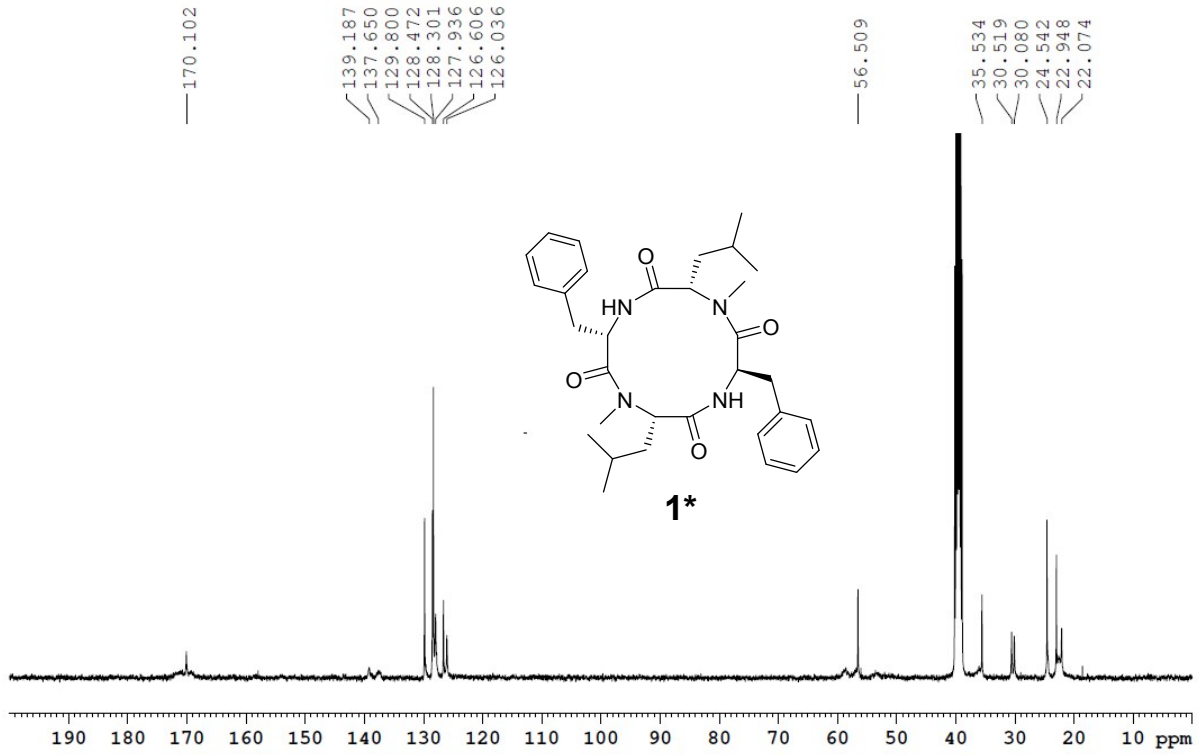

Figure S8 ^{13}C NMR spectrum of **1*** (DMSO-d_6, 298 K, 100 MHz).

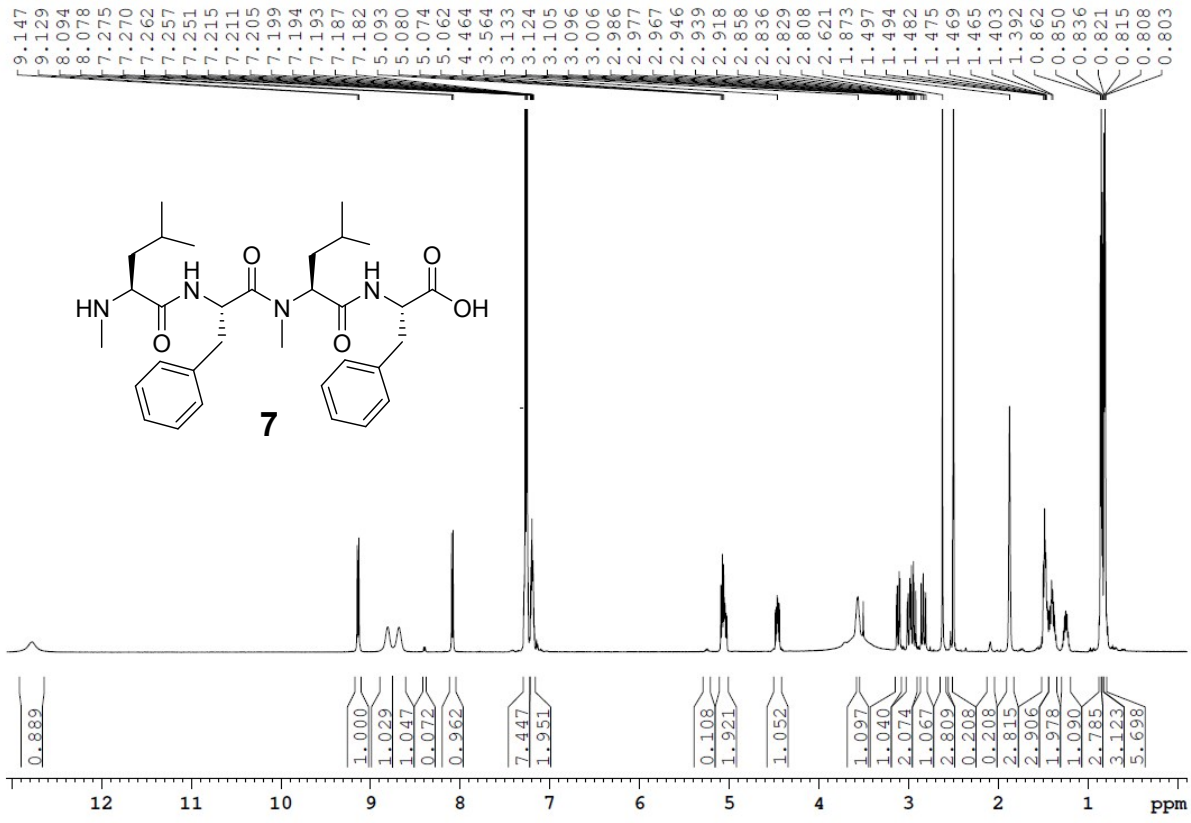

Figure S9: ^{1}H NMR spectrum of **7** (DMSO-d_6, 298 K, 500 MHz).

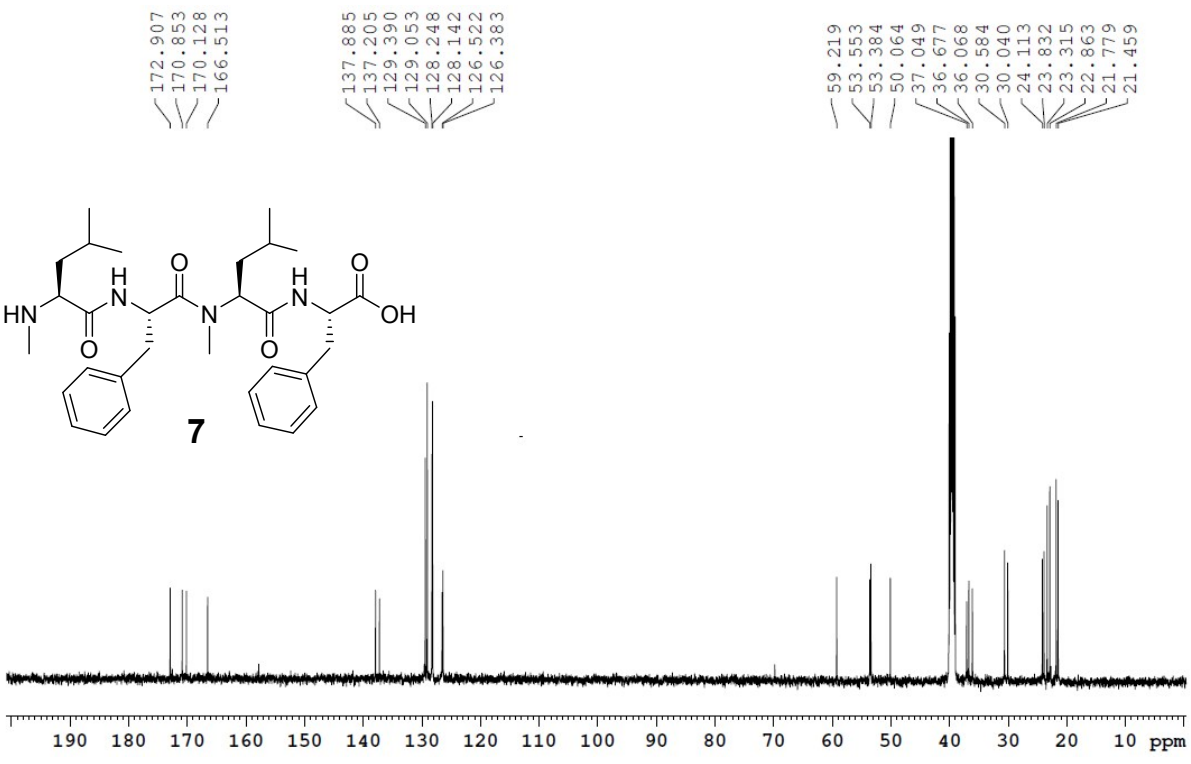

Figure S10 ^{13}C NMR spectrum of **7** (DMSO-d_6, 298 K, 125 MHz).

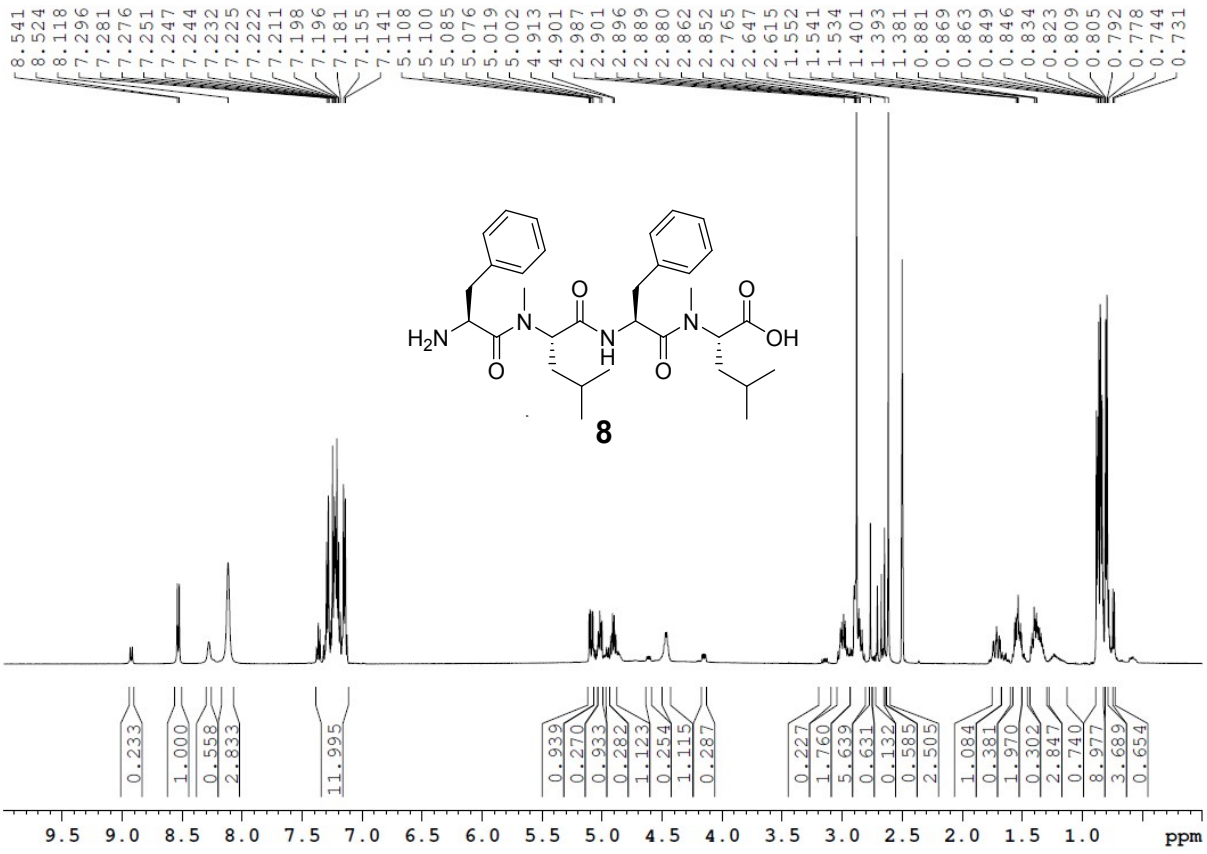

Figure S11: ^{1}H NMR spectrum of **8** (DMSO-d_6, 298 K, 500 MHz).

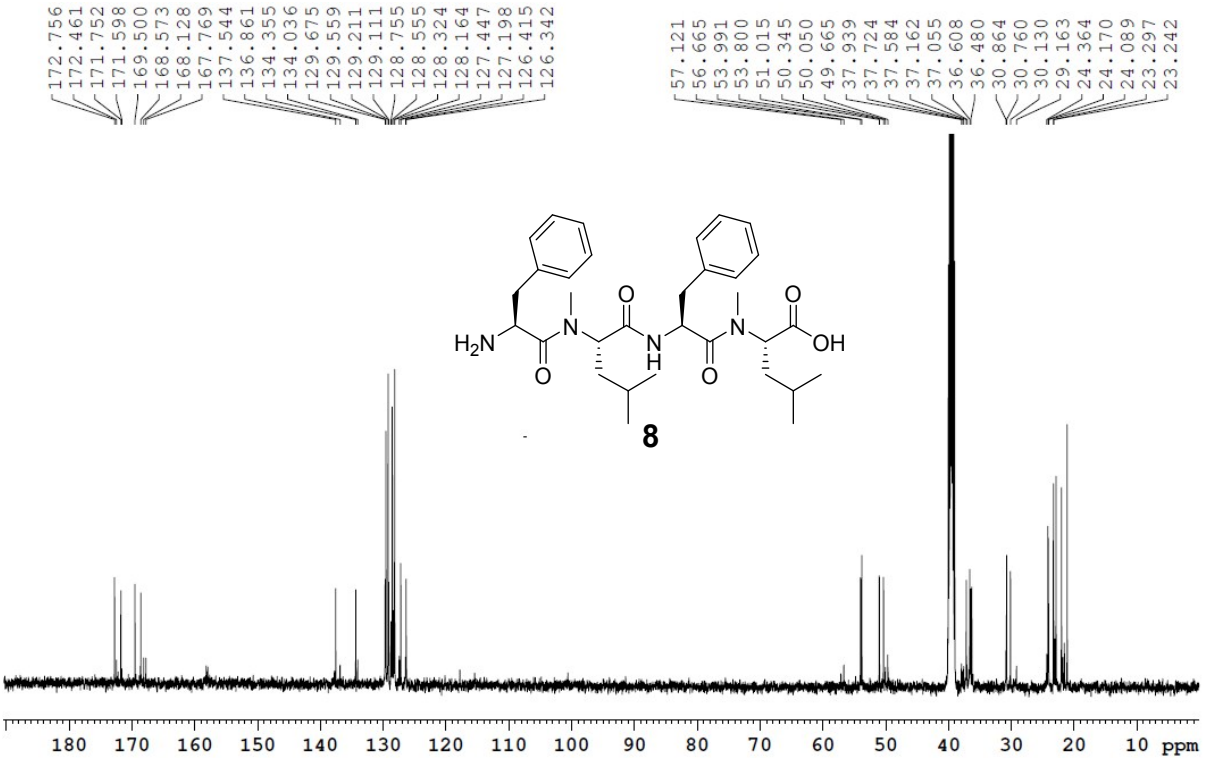

Figure S12 ^{13}C NMR spectrum of **8** (DMSO-d_6, 298 K, 125 MHz).

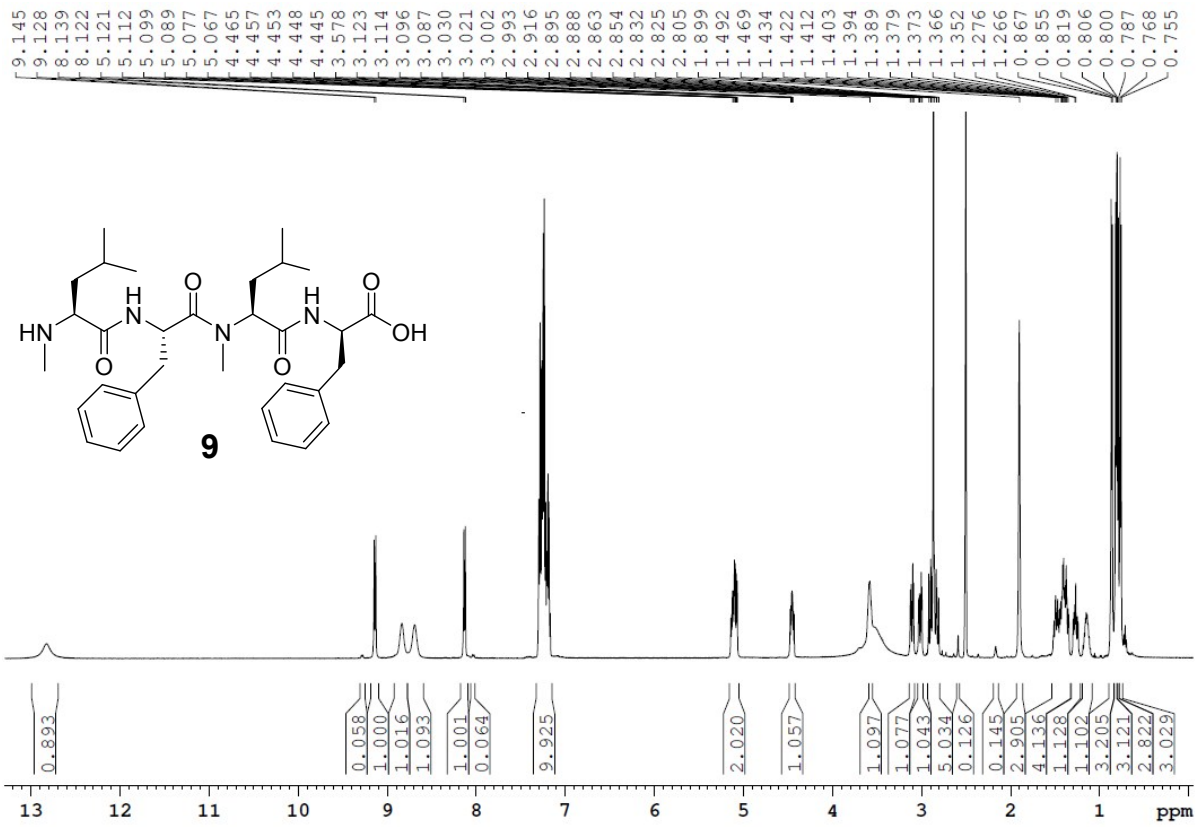

Figure S13: ^{1}H NMR spectrum of **9** (DMSO-d_6, 298 K, 500 MHz).

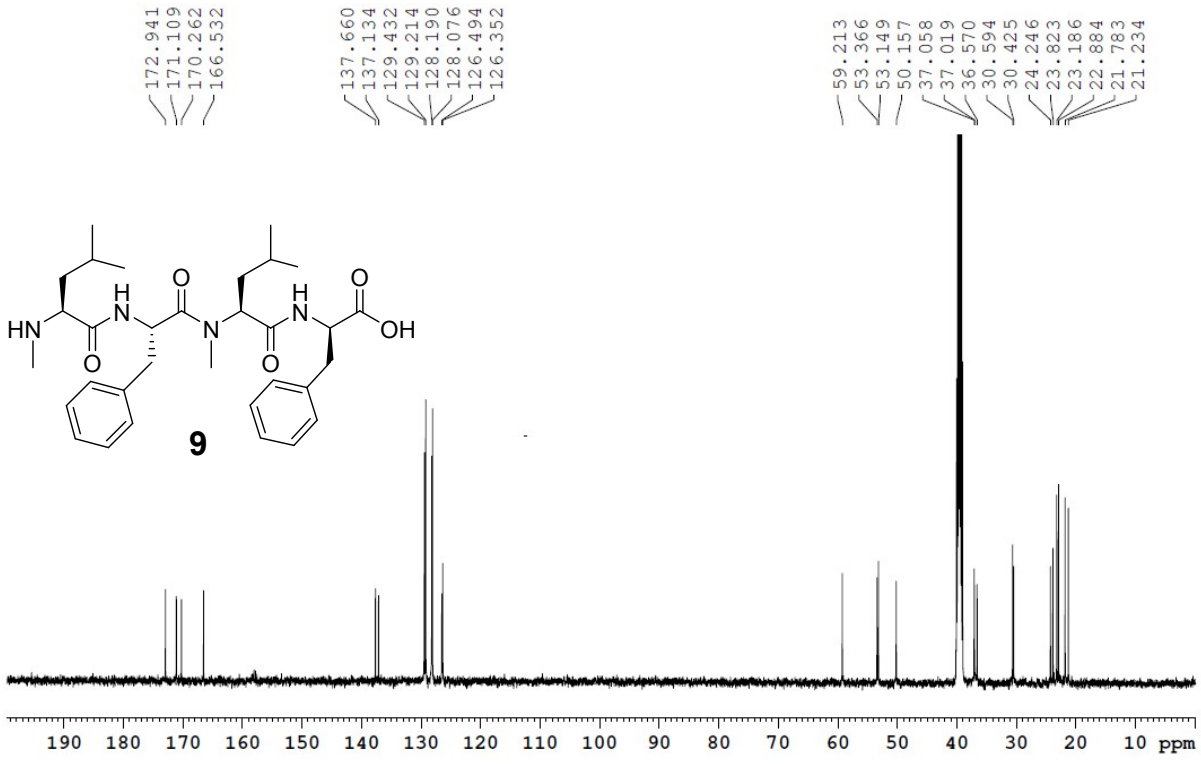

Figure S14 ^{13}C NMR spectrum of **9** (DMSO-d_6, 298 K, 125 MHz).

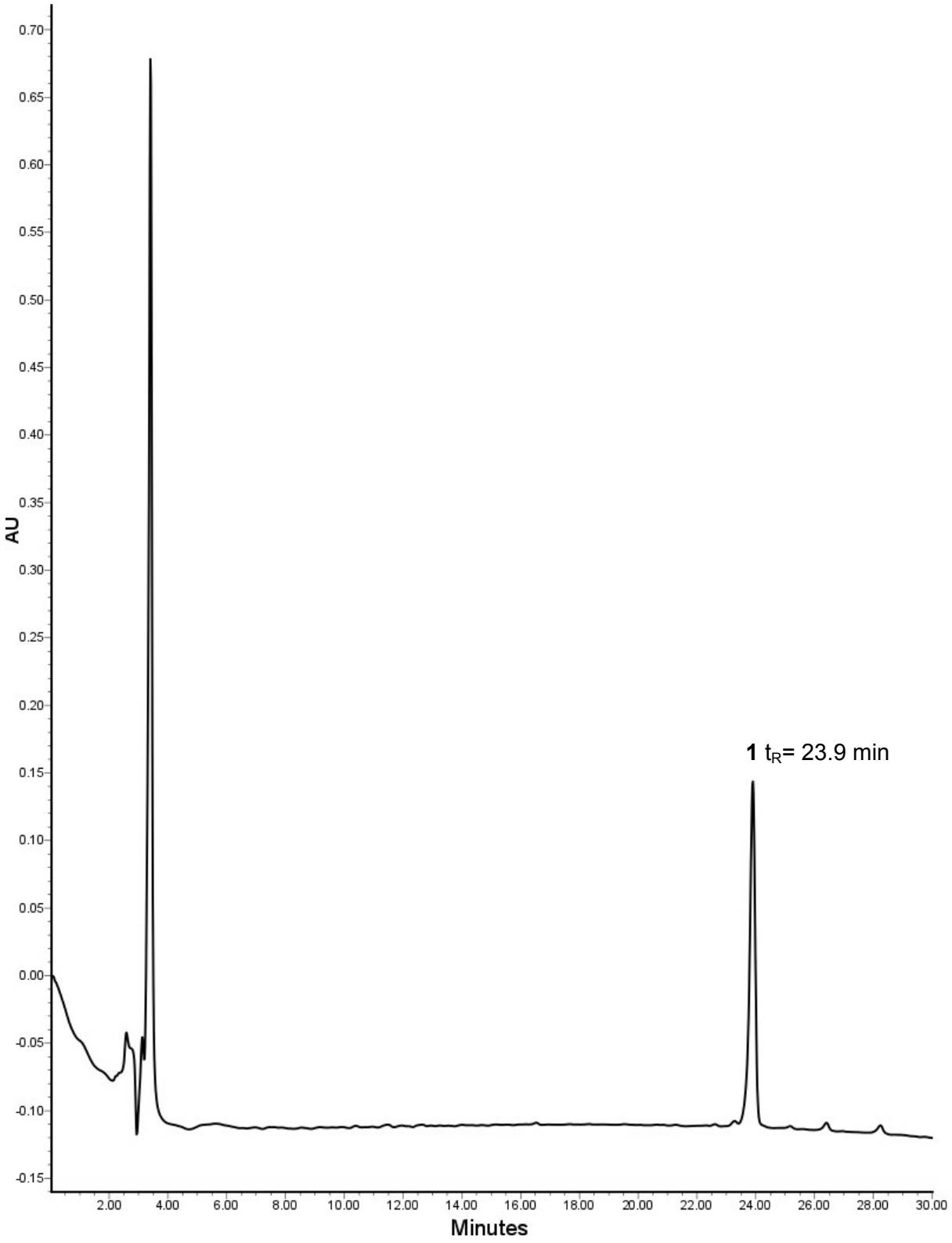

Figure S15: Analytical RP-HPLC chromatogram of purified **1**, 97 % purity (214 nm). Peaks with t_R < 4 min result from solvent spikes during injection.

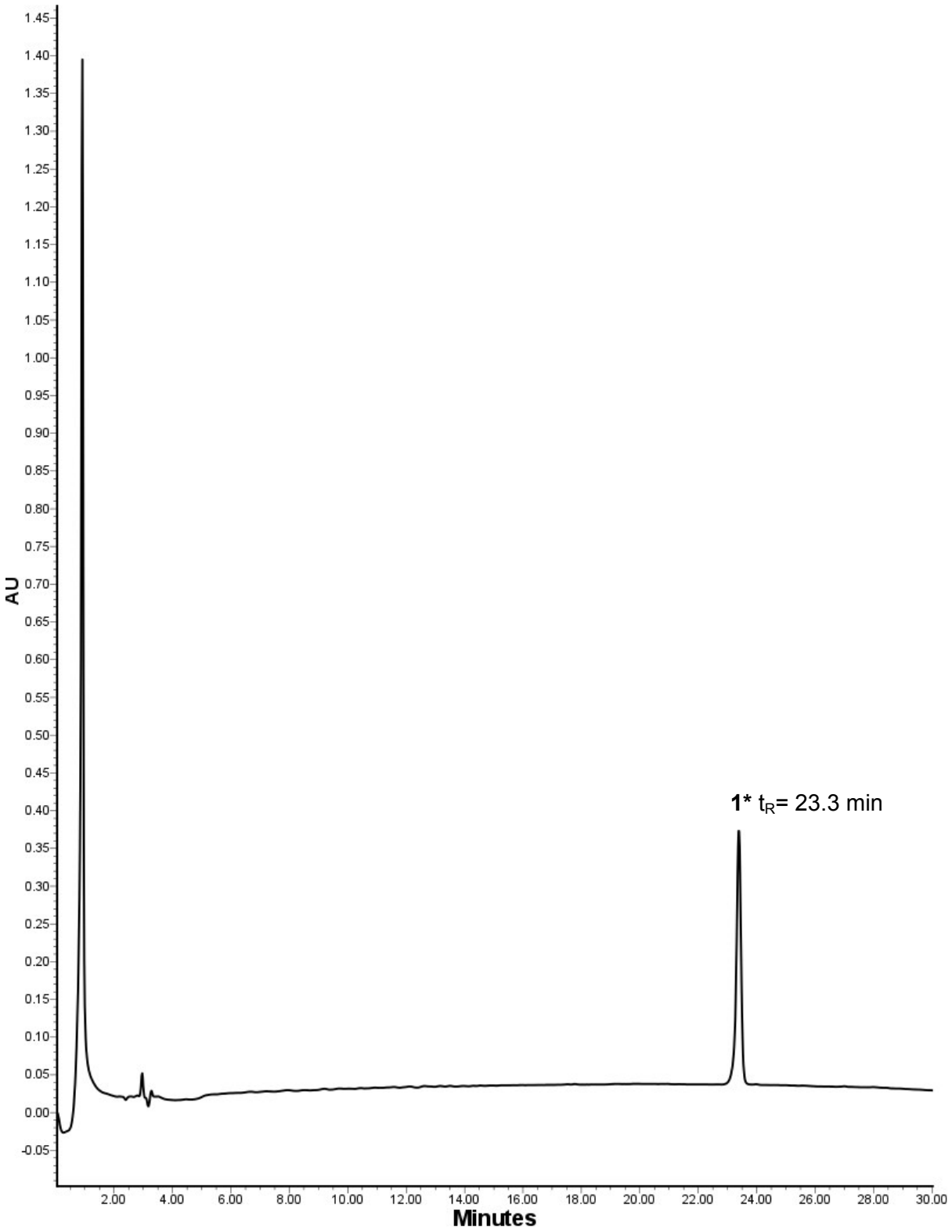

Figure S16: Analytical RP-HPLC chromatogram of purified **1***, > 99% purity (214 nm). Peaks with t_R < 4 min result from solvent spikes during injection.

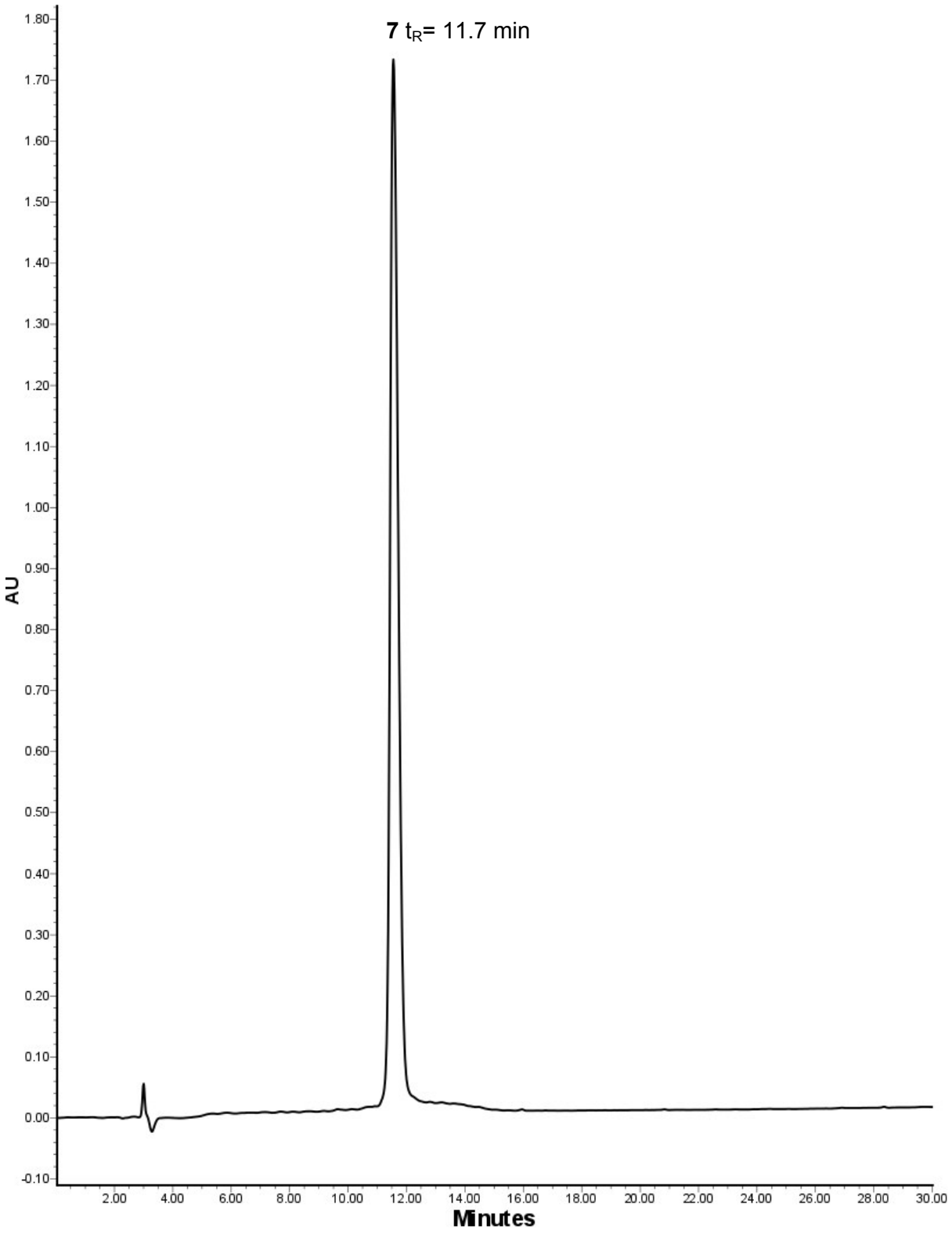

Figure S17: Analytical RP-HPLC chromatogram of purified **7**, > 99 % purity (214 nm). Peaks with t_R < 4 min result from solvent spikes during injection.

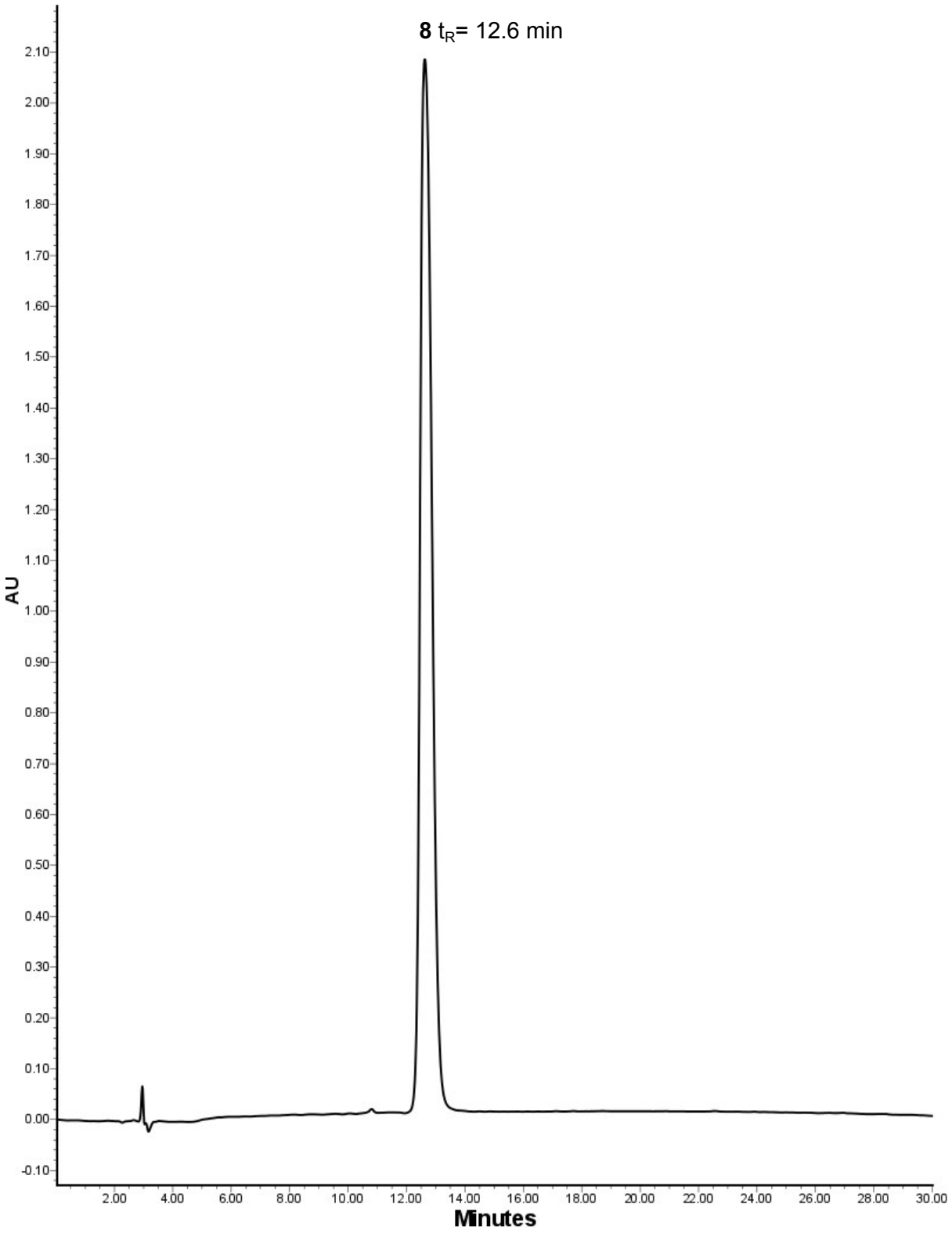

Figure S18: Analytical RP-HPLC chromatogram of purified **8**, > 99 % purity (214 nm). Peaks with t_R < 4 min result from solvent spikes during injection.

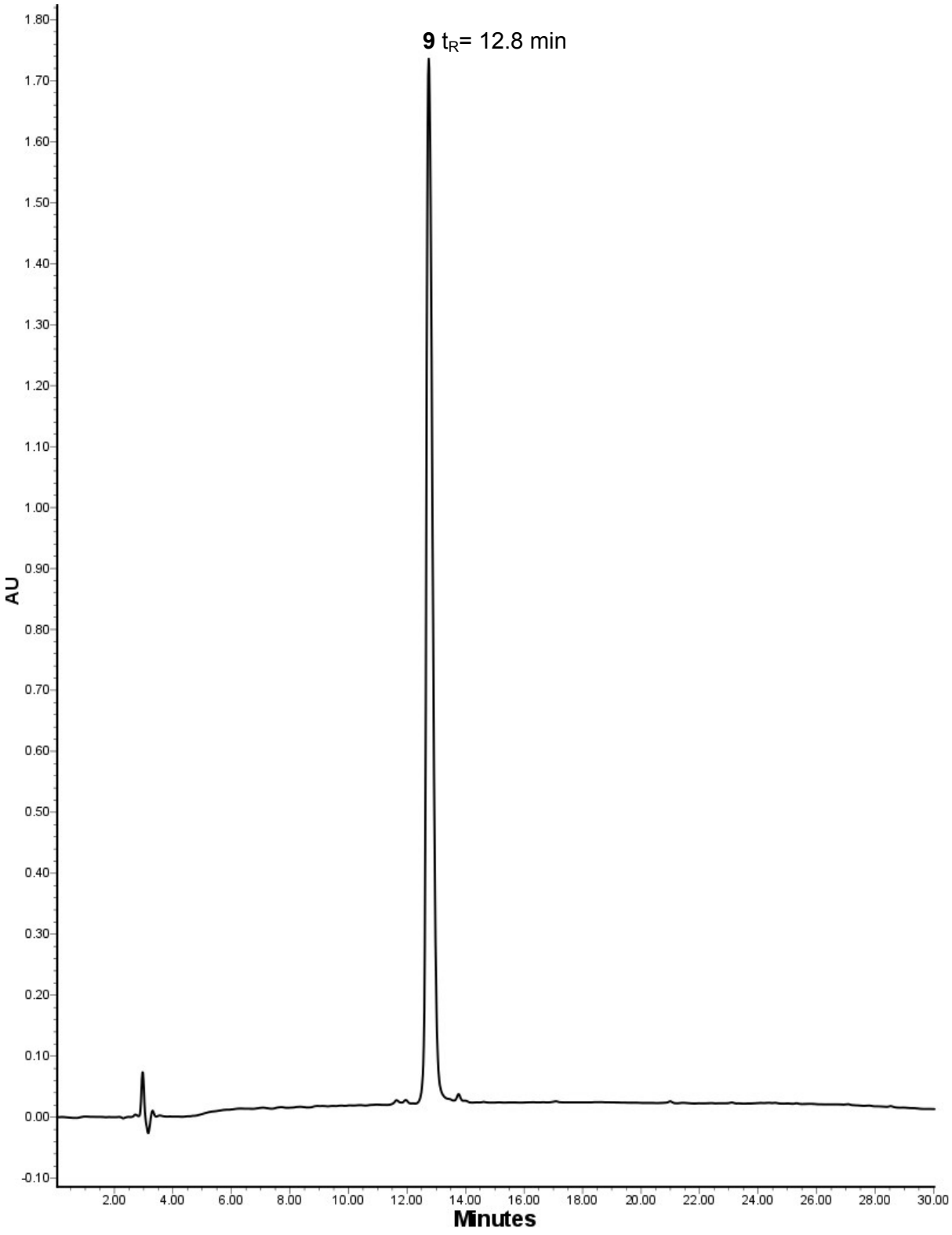

Figure S19: Analytical RP-HPLC chromatogram of purified **9**, > 99 % purity (214 nm). Peaks with t_R < 4 min result from solvent spikes during injection.

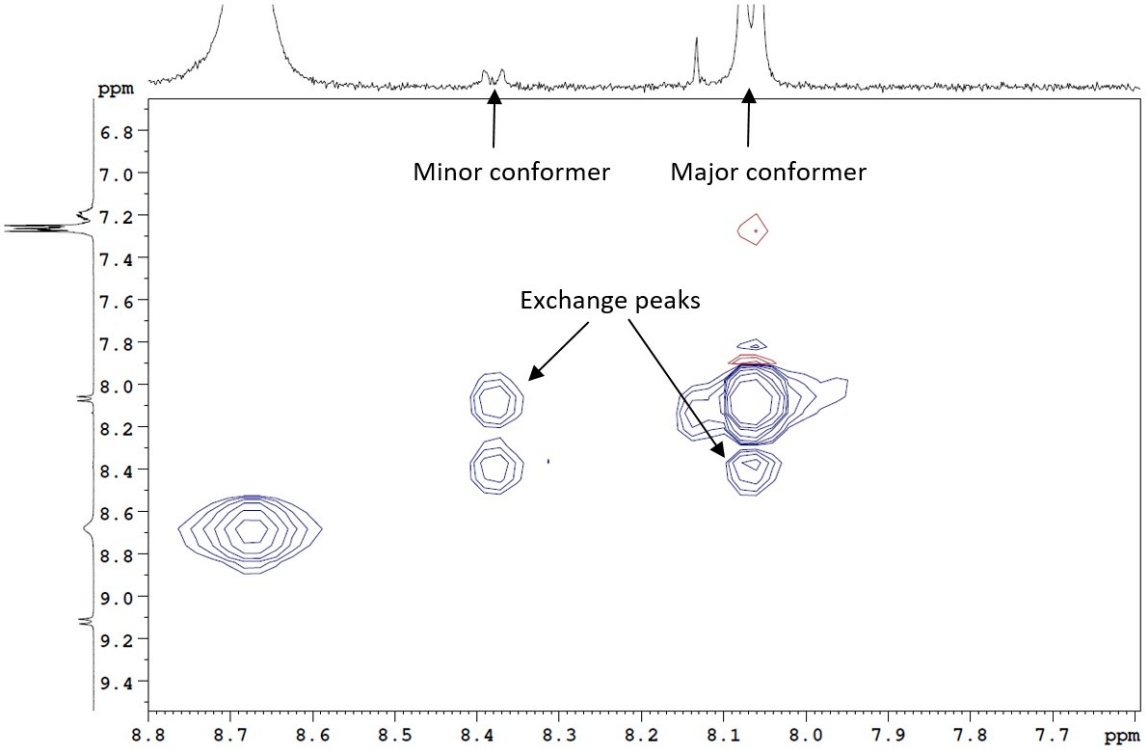

Figure S20: Partial NOESY spectrum (400 MHz) of **7** in DMSO-d_6 demonstrating exchange peaks between minor and major conformers. The minor conformer equates to approximately 11 %.

References

1. T. M. McPhillips, S. E. McPhillips, H.-J. Chiu, A. E. Cohen, A. M. Deacon, P. J. Ellis, E. Garman, A. Gonzalez, N. K. Sauter and R. P. Phizackerley, *J. Synchrotron Radiat.*, 2002, **9**, 401-406.
2. W. Kabsch, *Acta Crystallogr., Sect. D: Biol. Crystallogr*, 2010, **66**, 133-144.
3. G. M. Sheldrick, *Acta Crystallogr., Sect. A: Found. Adv.*, 2015, **71**, 3-8.
4. G. M. Sheldrick, *Acta Crystallogr., Sect. A: Found. Crystallogr.*, 2008, **64**, 112-122.
5. S. Zhang, R. L. M. De Leon, E. Lacey, A. M. Piggott, I. K. H. Leung and M. A. Brimble, *Eur. J. Org. Chem.*, 2017, **2017**, 149-158.
6. K. A. Fairweather, N. Sayyadi, I. J. Luck, J. K. Clegg and K. A. Jolliffe, *Org. Lett.*, 2010, **12**, 3136-3139.
7. M. El Haddadi, F. Cavelier, E. Vives, A. Azmani, J. Verducci and J. Martinez, *J. Pept. Sci.*, 2000, **6**, 560-570.
8. H. Guo, N. B. Kreuzenbeck, S. Otani, M. Garcia-Altares, H.-M. Dahse, C. Weigel, D. K. Aanen, C. Hertweck, M. Poulsen and C. Beemelmanns, *Org. Lett.*, 2016, **18**, 3338-3341.